Particle Accelerators
1976, Vol. 7, pp. 61–67

ALTERNATING PHASE FOCUSED LINACS

DONALD A. SWENSON†

Los Alamos Scientific Laboratory of the University of California, Los Alamos, New Mexico 87545, USA

(Received July 23, 1975; in final form September 15, 1975)

An array of alternating phase focused linac structures are presented which show promise for acceleration of protons and heavy ions at higher frequency and from lower energies than currently possible with magnetically focused drift tube linacs. In these structures, the transverse, as well as the longitudinal, focusing forces are produced by the rf fields. By arranging the drift tube lengths, and hence the gap positions, in an appropriate way, in a standing wave drift tube loaded structure, the particles can be made to experience acceleration and a succession of focusing and defocusing forces which result in satisfactory containment of the beam, without dependence on additional focusing fields. A scaling law is described which transforms the basic phase sequences to other synchronous energies, wavelengths, particle masses and charge states. A graphical parameter space is developed as an aid in selecting suitable basic phase sequences, and techniques are discussed for generating linacs. Three alternating phase focused linacs are presented as examples; one for protons, and the others for heavy ions. The geometry and performance of each are described.

1 INTRODUCTION

An array of alternating phase focused (APF) linac structures has been discovered which shows promise for acceleration of protons and heavy ions at higher frequencies and from lower energies than currently possible with the magnetic quadrupole focused drift tube linac structure. The available phase spaces in both the longitudinal and transverse planes are quite comparable to those of the latest generation of proton linacs. The acceleration rate is somewhat inferior to the conventional drift tube structure (down 30–40%) due to the investment of some of the accelerating potential in this new focusing role.

Particles which cross linac-type gaps at the peak of the accelerating voltage ($\phi = 0$) get the maximum acceleration possible, and little in the way of longitudinal or transverse focusing or defocusing. Particles which cross linac-type gaps at $\phi = -90°$ get no acceleration, but lots of longitudinal focusing and transverse defocusing, and particles which cross linac type gaps of $\phi = +90°$ get no acceleration, but lots of transverse focusing and longitudinal defocusing. Particles which cross gaps between these limits get varying amounts of acceleration, and longitudinal and transverse focusing and defocusing. By arranging the drift tube lengths, and hence gap positions, in an appropriate way, in a more or less conventional standing wave drift tube linac, the particles can be made to experience acceleration, and a succession of focusing and defocusing forces which result in satisfactory containment of the beam in the six-dimensional phase space without dependence on additional focusing fields. This means that drift tubes can be fabricated smaller and shorter than ever before, allowing the structure to be extended to higher frequencies and to lower energies than currently possible.

The possibility, tagged alternating phase focusing, was recognized soon after the discovery of the alternating gradient focusing.[1,2] Early investigations were restricted to symmetrical, and later assymmetrical, biperiodic phase sequences.[3–8] Many investigators concluded that the stable phase areas were small and of little practical interest. More recently, there has been a revival of interest in this focusing principle in connection with the high gradient prospects of superconducting structures, and the difficult focusing situations in heavy-ion linacs.[9–10] The Russians seem to have found some interesting structures in the late sixties and studies of these are in progress.[11–16]

The present development was prompted by an interest in extending the proton linac structure to higher field gradients, shorter wavelengths, and lower injection energies. All three of these factors compound dramatically the problem of practical fabrication of the magnetically focused drift tube structure.

† Work performed under the auspices of the U.S. Energy Research & Development Administration.

It was recognized that alternating phase focusing might provide a solution to these severe problems. Analytical studies in the past have not produced much to be enthusiastic about. The present approach is to seek an insight into the focusing principle by straightforward simulation of the beam dynamics of long structures with periodic gap phases. The basic properties of such structures can be most readily extracted by degrading the energy gain at each gap by the normal energy gain of the synchronous particle, thus producing structures which are strictly periodic in geometry as well as phases. Particles within the stable phase space of such pseudostructures execute closed oscillations around the synchronous particle which has a constant energy. Phase sequences that exhibit good focal properties in this periodic configuration should constitute good building blocks for practical linacs where the geometry changes as the particles accelerate.

A computer program was set up on the controls computer of LAMPF[17] to study the focal properties of these periodic pseudostructures for periodicities up to 8 gaps. The display and interaction capabilities of that system contributed significantly to the success of this investigation.

2 THE STRUCTURE

The basic period of the pseudostructure is completely defined by the kinetic (W) and rest (W_0) energies of the synchronous particle (constants), the wavelength of the rf, a field factor F related to the product of the average axial electric field E_0 and the transit time factor T, the number of gaps per period N_g, and the phase of the rf as the synchronous particle crosses each gap ϕ_n.

Although other possibilities exists, this report is restricted to structures where the distance between the n-1st and nth gap is

$$d_n = \frac{\phi_n - \phi_{n-1} + 2\pi}{2\pi} \beta\lambda.$$

Since the ϕ's are periodic, the average spacing between gaps is $\beta\lambda$.

The peak voltage on the nth gap, V_n, is taken to be the product of the average axial electric field, E_0, and the average value of d_n and d_{n+1}.

3 DYNAMICS

The transverse dynamics has circular symmetry, making it sufficient to study either transverse plane. The xx' dynamics is dependent on only two equations; one giving the change in x during the drift between gaps, and the other giving the change in x' at the gap. These equations for the nth drift and gap are:

$$\Delta x = d_n x' \tag{1}$$

$$\Delta x' = \frac{-\pi q V_n T \sin \phi_n}{W_0 \beta^3 \gamma^3 \lambda} x \tag{2}$$

where β and γ are the relativistic velocity and mass factors corresponding to the energy of the particle during the nth drift, and ϕ_n is the phase of the rf when it arrives at the nth gap.

The longitudinal dynamics is dependent on only two equations; one giving the change in the phase coordinate during the drift between gaps, and the other giving the relative change in the energy of the particle and the synchronous particle at the gap. These equations for the nth drift and gap are:

$$\Delta\phi = 2\pi\left[\frac{d_n}{\beta_s \lambda}\frac{\beta_s}{\beta} - 1\right] \tag{3}$$

$$\Delta W = q V_n T(\cos\phi - \cos\phi_n) \tag{4}$$

The transverse dynamics is more strongly coupled to the longitudinal dynamics than in the conventional magnetically focused linac.[18] Dreval, Kushin and Mokhov have studied the longitudinal-to-transverse coupling effects[13] and the transverse space-charge effects[16] for their asymmetric variable-phase focused structure. They note potentially serious problems, but conclude that, given proper attention to these problems, their structure should be able to handle currents of 100 mA or higher up to energies of 100 MeV. Studies of these important effects by the author are in progress.

4 THE SCALING LAW

The β_s/β term in Eq. (3) can be expressed approximately as $1 - \delta W/\beta_s^2\gamma_s^3 W_0$ where δW is the energy excursion $W - W_s$. If structure lengths scale as $\beta_s\lambda$ and gap voltages scale as $\beta_s^2\gamma_s^3 W_0/q$, one notes that energy excursions go as $\beta_s^2\gamma_s^3 W_0$ while the phase excursions are independent of scaling, and the x' excursions go as $1/\beta_s\lambda$ while the x excursions are independent of scaling. The scaling implies that E_0 scales like $\beta_s\gamma_s^3 W_0/q$.

The area enclosed by the largest stable longitudinal oscillation goes as $\beta^2\gamma^3$. The area (in the

canonical variables x and p_x) enclosed by the transverse oscillation of a given transverse excursion goes as $\beta\gamma$ time $1/\beta\lambda$ or as γ/λ.

5 THE ARRAY

Since the scaling law can be used to transform any basic sequence and excitation to a different synchronous energy, a different wavelength, a different rest mass or a different charge state, the studies are presented here for the nominal values of $W_s = 1$ MeV, $\lambda = 0.75$ meters (400 MHz), and for the rest mass and charge state of a proton.

The excitation and transit time factor for these nominal parameters is referred to as a field factor F, to avoid confusion with the actual value of the product $E_0 T$ after scaling. $E_0 T$ is related to F by

$$E_0 T = \frac{\beta\gamma^3 W_0/q\lambda}{\beta_n\gamma_n^3 W_{0,n}/q_n\lambda_n} F$$

where the subscript n implies the nominal values listed above.

Sixteen basic sequences are presented in Figure 1, ranging from two-gap periodicities at the top to eight-gap periodicities at the bottom. Each sequence has a characteristic acceleration factor which is the average value of $V_n \cos\phi_n/E_0\beta\lambda$ over the gaps of the sequence. Within each periodicity, the sequences are arranged in order of decreasing acceleration factor. To the right of each sequence, there are a number of dots corresponding to suitable excitations for the sequence ranging from 0 to 16 MV/m. The asterisks represent the excitations that exhibit the maximum longitudinal stability. The two columns on the right side of the figure give the normalized emittance ($\beta\gamma ab$) of a beam whose maximum diameter is 1 cm, and the total widths of the longitudinal acceptance.

Two things are immediately obvious from this array of sequences:

1) The range of suitable excitations for a given sequence is relatively narrow, and

2) The optimum excitation of the sequences decreases as periodicity increases.

Figure 2 shows an example of the graphical output from which these results were extracted. Such outputs were studied for each sequence and

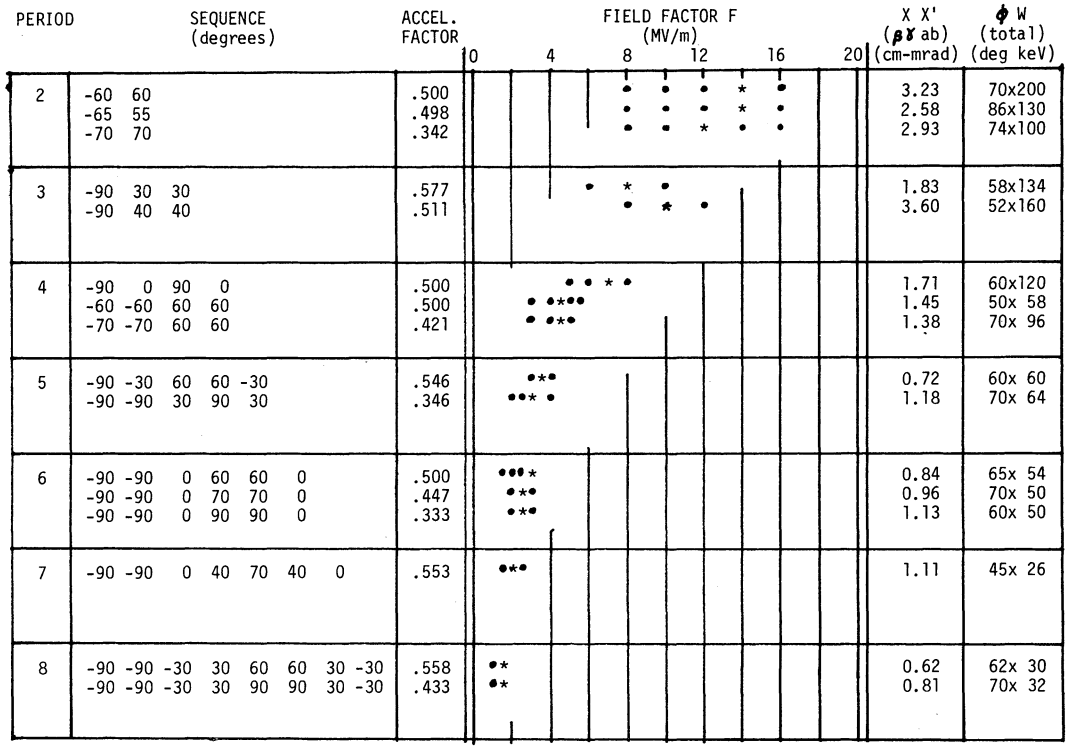

FIGURE 1 Array of basic phase sequences with excitation and performance data.

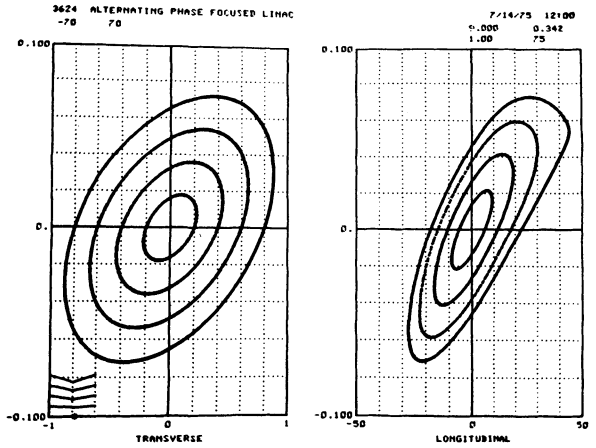

FIGURE 2 Graphical output for one phase sequence and excitation showing stable oscillations in both the transverse and longitudinal plane.

excitation presented in Figure 1, and for hundreds of other sequences and excitations that were definitely inferior to those presented.

6 PRACTICAL APF LINAC DESIGN

Given the insight that these studies of the basic sequences provide, the next step is to develop a procedure for using these results to generate practical APF linacs in which the acceleration process is allowed to develop.

The scaling law provides guidance for transforming the dots on Figure 1 to other energies and other frequencies. Rearranging the relation between F and E_0, one gets

$$F \cdot \beta\gamma^3 = \frac{\beta_n \gamma_n^3}{\lambda_n} E_0 \lambda C = 0.0617 E_0 T \lambda C$$

where $C = (q/W_0)/(q_n/W_{0,n})$ is the charge per nucleon as compared to the proton. It is convenient to define an F, $\beta\gamma^3$ space as shown in Figure 3, where the hyperbolae are lines of constant $E_0 T\lambda C$.

Structure economies and physical limitations would seem to bracket the range of E_0's of interest. Likewise, the range of λ is bracketed by rf power considerations and beam and cavity dimensions, T is a function of β, λ and bore radius, and C is determined by the choice of projectile, and in the case of heavy ions, the resulting charge state. Consequently, $E_0 T\lambda C$ is a quantity that tends to be reasonably well bracketed in the early stage of the design process. It forms a hyperbolic band in the F, $\beta\gamma^3$ space.

Horizontal (sequence) bands which intersect the hyperbolic ($E_0 T\lambda C$) band within the range of $\beta\gamma^3$ of interest, are candidates for use. The F, $\beta\gamma^3$ space graphically demonstrates the basic sequences and excitations applicable to given accelerator applications.

For example, a 400 MHz ($\lambda = 0.75$ meters) proton linac with $E_0 T$ at or below 4 MV/meter is constrained to the region below the $E_0 T\lambda C$ hyperbola for 3 MV. Dropping too far below this excitation may result in excessive accelerator length. The design might therefore be constrained to the hyperbolic band between the hyperbolae for 2 and 3 MV. Acceleration from 250 keV to 10 MeV suggests the need to employ several basic sequences in order to span the indicated range of horizontal parameter.

The easiest way to concoct a practical APF linac from the building blocks of Figure 1 is to adopt a favorable sequence and F value, and scale it precisely according to the scaling law. This implies tilting $E_0 T$ as $\beta\gamma^3$, which for long structure may imply too low a field in the beginning or too high a field at the end. Table I describes an 18-cell, 400 MHz linac designed in this way, which accelerates protons from 250 keV to 3.2 MeV in a distance of 62 cm. The electric field varies from 4.5 MV/m at the input end to 13.2 MV/m at the output end. Figure 4 shows the longitudinal section of this linac.

The transverse and longitudinal acceptances of this short linac are shown in Figure 5. The transverse emittance of a one-centimeter-diameter beam at the injection energy is 35π cm-mrad (area), which corresponds to a normalized emittance ($\beta\gamma ab$) of 0.81 cm-mrad. The longitudinal acceptance has total widths of 90° and 60 keV.

The next easiest way to concoct a practical APF linac is to adopt a favorable sequence and F value for the low energy end of interest, and scale it according to the scaling law until the fields reach some practical limit, after which the fields are bounded at that limit. This implies a droop in F value after the electric fields have limited, but in many cases, suitable performance is observed. Limiting the fields in the example above to 10 MV/m has only minor effects on the performance.

Many other schemes can be conceived where one sequence is scaled until the fields reach the practical limit, at which time another sequence with a lower F value is introduced and scaled, etc.

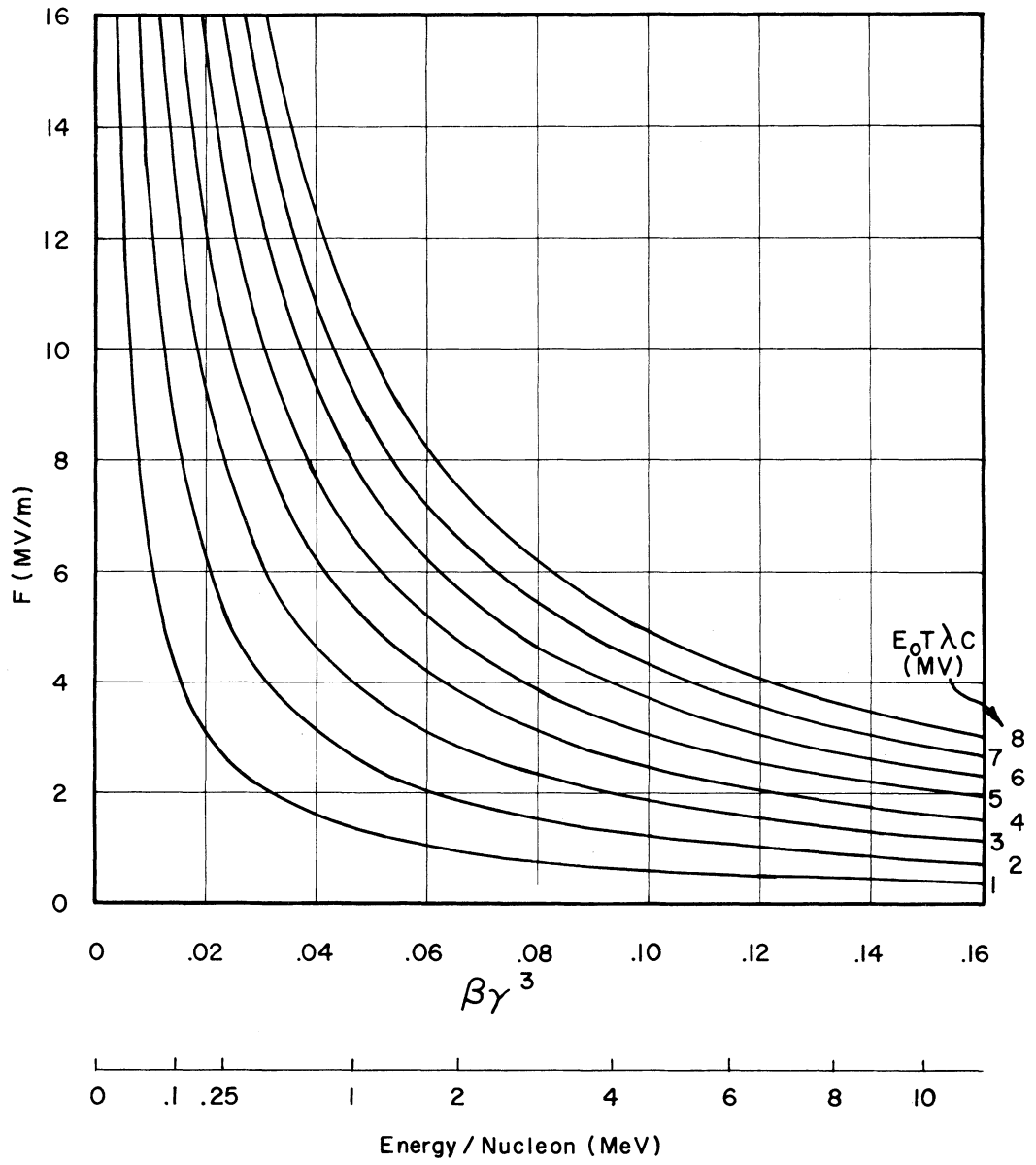

FIGURE 3 The F, $\beta\gamma^3$ space with hyperbolae of constant $E_0 T\lambda C$.

Abrupt changes in periodicity suggest the need for "matching," which is not addressed here.

Smooth changes can be imagined where one moves smoothly from one sequence to another of the same periodicity by gradually changing the magnitudes of the phases. Such a technique might be used to convert from an initial sequence with a large longitudinal acceptance and a poor acceleration factor, to one with a better acceleration factor at the expense of the longitudinal focusing, which otherwise grows rapidly as $\beta^2\gamma^3$.

And finally, of course, one may find algorithms for concocting APF linacs which are not based on the building blocks of Figure 1, but which draw only from the general understanding that they provide.

TABLE I

An 18-cell, 400-MHz, APF linac for protons

Projectile: Proton
Injection energy: 0.25 MeV
Final energy: 3.19 MeV
Total length: 62.5 cm
Transverse acceptance ($\beta\gamma ab$ for 1-cm-diam beam): 0.81 cm-mrad
Longitudinal acceptance (total widths): 90° × 60 kV

Cell Number	Phase (°)	E_0 (MV/m)	Energy (MeV)	Beta	Cell length	Total length
1	30	4.158	0.303	0.025	1.645	1.645
2	−90	4.581	0.303	0.025	1.907	3.552
3	30	4.581	0.387	0.029	2.348	5.900
4	30	5.176	0.462	0.031	1.862	7.762
5	−90	5.657	0.462	0.031	2.354	10.115
6	30	5.657	0.590	0.035	2.899	13.014
7	30	6.394	0.705	0.039	2.298	15.312
8	−90	6.989	0.705	0.039	2.906	18.217
9	30	6.989	0.900	0.044	3.578	21.795
10	30	7.900	1.074	0.048	2.837	24.632
11	−90	8.889	1.074	0.048	3.589	28.218
12	30	8.889	1.372	0.054	4.417	32.636
13	30	9.766	1.639	0.059	3.501	36.136
14	−90	10.680	1.639	0.059	4.427	40.563
15	30	10.680	2.093	0.067	5.451	46.014
16	30	12.082	2.500	0.073	4.322	50.336
17	−90	13.218	2.500	0.073	5.470	55.800
18	30	13.218	3.193	0.082	6.728	62.528

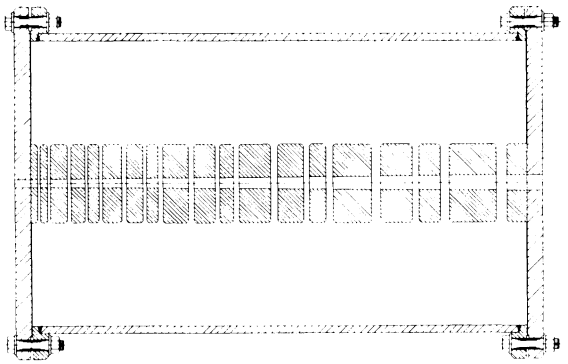

FIGURE 4 Longitudinal section of linac described in Table I. Total length = 62 cm.

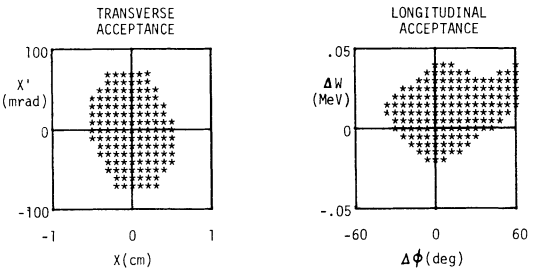

FIGURE 5 Transverse and longitudinal acceptances of linac described in Table I.

7 HEAVY ION ACCELERATION

From the point of view of acceleration and beam dynamics, heavy ions differ from protons by only the factor C, the charge per nucleon as compared to the proton. This factor is unity for protons, and considerably less than unity for heavy ions.

The injection energy per nucleon (MeV) is C times the injector voltage (MV). The final energies of heavy ion accelerators are often expressed in MeV/nucleon. The horizontal scale of the F, $\beta\gamma^3$ space can be used for heavy ion linac design by interpreting the energy scale as energy per nucleon. In general, heavy ion linacs deal with smaller values of energy per nucleon than normal for proton linacs.

For the same E_0T's and λ's, the $E_0T\lambda C$ hyperbolae lie considerably closer to the origin for heavy

TABLE II

A 40-cell, 200-MHz, APF linac for heavy ions

Projectile: Tin ion $^{124}Sn(+9)$
Injection voltage: 1.0 MV
Injection energy: 0.072 MeV/nucleon
Final energy: 0.285 MeV/nucleon
Total length: 107 cm
Transverse acceptance ($\beta\gamma ab$ for 2-cm-diam beam): 0.37 cm-mrad
Longitudinal acceptance (total widths): 60° × 80 kV
Phase sequence: 60 30 −30 −90 −90 −30 30 60
E_0 (MV/m): 3.7 to 7.2
Shortest cell: 1.63 cm

ion applications than for proton linac applications.

These effects combine to force heavy ion linac design into the range of smaller F values, and hence longer periodicities. Table II describes a 200-MHz linac designed to accelerate $^{124}Sn(+9)$ from a 1-MV terminal (0.072 MeV/nucleon) to 0.285 MeV/nucleon in a length of about one meter.

Table III describes a 70-MHz linac which accelerates $^{238}U(+7)$ from a 400-kV terminal (0.012 MeV/nucleon) to 0.105 MeV/nucleon in a length of about two meters.

TABLE III

A 48-cell, 70-MHz, APF linac for heavy ions

Projectile: Uranium ion $^{238}U(+7)$
Injection voltage: 400 kV
Injection energy: 0.012 MeV/nucleon
Final energy: 0.105 MeV/nucleon
Total length: 193 cm
Transverse acceptance ($\beta\gamma ab$ for 2-cm-diam beam): 0.20 cm-mrad
Longitudinal acceptance (total widths): 70° × 60 kV
Phase sequence: 60 0 −90 −90 0 60
E_0 (MV/m): 2.04 to 4.0
Shortest cell: 1.81 cm

CONCLUSIONS

These developments would seem to make low-energy protons more readily available from relatively modest facilities. For higher energy applications, these developments would seem to offer an important bridge between a few hundred keV and a few tens of MeV, where the chore of acceleration of the well bunched and focused beam could be taken over by a quadrupole-focused drift-tube linac of higher frequency and higher gradient than normal.

The low velocity capabilities of these structures are ideally suited to heavy-ion applications.

There may also be some applications of these structures to the problem of bunching and focusing electrons in the klystrons.[19]

The author is indebted to Ken Crandall and Bob Gluckstern for their participation in the early stage of this development, and to Crandall, Gluckstern, E. Knapp, D. Hagerman, R. Jameson and J. Stovall for subsequent discussion and encouragement.

REFERENCES

1. E. D. Courant, M. S. Livingston, and H. S. Snyder, *Phys. Rev.*, **88**, 1190 (1952).
2. N. Christofilos, U.S. Patent No. 2,736,799 (filed 1950).
3. M. L. Good, *Phys. Rev.*, **92**, 538 (1953).
4. L. B. Mullett, AERE GP/M 147, 1953 (unpublished report).
5. Ia. B. Fainberg, *Proceedings CERN Symposium on High Energy Accelerators and Pion Physics, 1956*, p. 91.
6. A. D. Vlasov, *Theory of Linear Accelerators*, Moscow, 1965, and (English translation) Jerusalem, 1968.
7. G. Teissier, A. Chabert, B. Veyron, LYCEN/6528, Lyon, 1966 (unpublished report).
8. D. Boussard, "Radiofrequency Focusing in Heavy Ion Linear Accelerators," in *Linear Accelerators*, P. Lapostolle and A. Septier, Eds., North Holland, Amsterdam, 1970.
9. E. E. Chambers, HEPL 653, Stanford University, 1971 (unpublished report).
10. A. J. Sierk, C. J. Hamer, and T. A. Tombrello, *Particle Accelerators*, **2**, 149 (1971).
11. V. V. Kushin, *Atomnaya Energia*, Vol. 29, 2, 1970, p. 123.
12. B. P. Murin, *Proceedings 8th International Conference on High Energy Accelerators, CERN, 1971*, p. 540.
13. I. D. Dreval and V. V. Kushin, *Journal of Technical Physics*, Vol. 42, 1972, p. 1915.
14. V. V. Kushin, B. T. Zarubin, V. V. Svirin, N. M. Chistiakova, *Pribory i Tekhnika Eksperimenta*, No. 6, p. 15 (1972), also English translation, *Instruments and Experimental Techniques*, **15**, 1628 (1972).
15. V. V. Kushin, personal communication.
16. I. D. Dreval, V. V. Kushin, and V. M. Mokhov, *Journal of Technical Physics*, Vol. 43, 1973, p. 1950.
17. H. S. Butler, *Proceedings III All Union National Particle Accelerator Conference, Moscow, 1972*, Vol. II, p. 46.
18. R. L. Gluckstern, personal communication.
19. T. J. Boyd, personal communication.